Theory of time-dependent plastic deformation in disordered solids

B. N. J. Persson
Institut für Festkörperforschung, Forschungszentrum Jülich, D-52425 Jülich, Germany
(Received 26 February 1999; revised manuscript received 18 August 1999)

I present a theory of time-dependent plastic deformation of solids. I derive a general equation of motion for the stress probability distribution function *P*. I consider in detail uniaxial tension and show how this case can be (approximately) mapped onto a simple one-dimensional spring-block model. I study stationary creep and the linear and nonlinear response of a solid block to an imposed oscillatory strain. The theory is in good agreement with experimental data.

I. INTRODUCTION

In this paper I develop a theory of time-dependent plastic deformation, which should be valid for a large class of disordered materials. The theory is based on the concept of a stress probability distribution function *P*, which, at a given time, is determined by the external stress and temperature fields the body has been exposed to at all earlier times. The basic idea behind this approach is that a solid that has been exposed to external stresses in the past will have an internal stress distribution (residual stress), which varies rapidly in space (perhaps on the length scale of ~10–100 Å in a glassy solid) and slowly in time. The yield stress of a solid, for example, depends on this internal stress distribution *P*, and will, even in the absence of external stresses, evolve slowly (because of thermal excitation over the local barriers) with increasing time. One implication of this formalism is that while the (ensemble) average stress in a solid usually vanishes when the solid is not exposed to external stresses, i.e.,

$$\langle \sigma_{ij} \rangle = \int d\sigma \, \sigma_{ij} P = 0,$$

the quantity $\langle \sigma_{ij} \sigma_{ij} \rangle$ does in general not vanish.

In analogy with the well-known equation of state of a perfect gas, simple theories of plastic deformation often specify ''mechanical equations of state.'' [1] Such a state equation takes the form $F(\sigma, \varepsilon, \dot{\varepsilon}, T) = 0$, and depends only on the mean stress $\langle \sigma \rangle$, usually written as σ for simplicity, the strain ε, the strain rate $\dot{\varepsilon}$, and the temperature *T*. In this type of model, the stress in a solid at an arbitrary time *t*, depends only on the external applied stresses at the same time *t*, i.e., there is no information about the history of the external stresses the block has been exposed to. Such relations are well defined under some conditions, e.g., if a solid block is (slowly) elongated (uniaxial tension) at a constant strain rate, a steady state may be reached after some time where the stress distribution *P* takes a unique (fixed-point) form, which is independent of the initial conditions. In this case a definite well-defined relation will occur between the instantaneous values of the quantities introduced above, see Eqs. (36)–(38) below. However, it is usually not possible to describe the time-dependent deformation of a solid by a relation of the form $F(\sigma, \varepsilon, \dot{\varepsilon}, T) = 0$, since the relation between the stress and strain at time *t* depends in general on the history of the external stress and temperature fields the solid has been exposed to. On the other hand, the formalism of the present paper does take into account these memory effects via the distribution function *P*. Another approach to take into account memory effects is to introduce *state variables* Ψ_α, which are determined by equations of motion that depend on the stress and temperature fields the block has been exposed to at earlier times. This type of approach has been found to be very useful in the context of sliding friction[2] where, e.g., the static friction force depends on the time of stationary contact, and may also be very useful in the context of time-dependent plastic deformation. In fact, attempts to introduce such state variables for plastic deformation have already been presented by Argon *et al.*[3] and by Falk and Langer.[4]

I would like to emphasize that the present theory is not valid for single crystals, but assumes glassy atomic solids. It may also tentatively be applied to strongly plastically deformed solids and alloys. In the latter two cases, plastic deformation can be considered as resulting from elementary slip processes where short segments of dislocations move short distances before getting pinned by crystal imperfections (e.g., other dislocations, impurities or alloy atoms). For these systems, the stress probability distribution function *P* can be considered as resulting from an ensemble of macroscopically identical solids but with different internal distribution of dislocations and pinning centers. For glassy solids the local yield processes may be more complex than in materials with more long-range crystalline order, but the basic idea is the same. The theory presented below is of a mean-field type. Thus the stress that acts on a stress block from the surrounding stress blocks is only taken into account in an average sense. However, this approach has been found accurate in an earlier study[5] of a one-dimensional model, which was solved both exactly (using computer simulations) and within a mean-field approximation, similar to the one developed in the present paper for three-dimensional systems. The mean-field approximation employed in the present case may, in fact, be even more accurate than in the one-dimensional case, since mean-field approximations usually work much better in higher dimensional systems because of the increased number of nearest neighbors (see, e.g., Ref. 6).

There has been some earlier work on the theory of time-dependent plastic deformation along the lines of the present paper. Most similar to the present approach is a theory of Argon *et al.*,[3] who have studied plastic deformation in glassy

polymers by mesoscopic simulations. They assumed that plastic deformation is associated with local stochastic shear transformations, at a rate governed by a characteristic energy barrier. The total stress includes not only the applied stress, but all other preexisting disorder-related internal misfit stresses, as well as the total sum of the elastic interactions with other past and present shear transformations, external to the transformation considered specifically. This theory is a numerical procedure and has only been applied to two-dimensional systems. Other studies of the role of fluctuating internal stresses on plastic flow have been presented by Egami and Vitek,[7] and by Bulatov and Suter.[8] These studies have developed specific thermally activated deformation models that were stimulated by experiments, and are in good agreement with much experimental work on plastic flow of glassy metals and polymer glasses.

The present theory is similar in spirit to that of Argon *et al.*,[3] but it is based on dynamical equations, and has the advantage that analytical results can be obtained in various limiting cases. We present a complete set of equations for time-dependent plastic deformation and a few illustrative applications. In Sec. II I derive a general equation of motion for the stress probability distribution function P. I consider in detail uniaxial tension (Sec. III) and show how this case can be (approximately) mapped on a simple one-dimensional spring-block model (Sec. IV). I study stationary creep in Sec. V and linear and nonlinear response of a solid block to imposed oscillatory strain in Secs. VI and VII. Section VIII describes relaxation and recovery phenomena in plastic deformation. Section IX presents some mathematical developments and illustrations. Section X presents a few comments, and in Sec. XI the theory is compared with experimental data.

II. GENERAL THEORY

When a solid block is exposed to large external stresses, plastic deformation usually occurs. Consider a block placed on a substrate. In this case plastic deformation occurs at the contact areas, and a short time after contact the local stresses equal the plastic yield stress. Plastic deformation can be considered as resulting from shear yielding of small volume elements (stress blocks) resulting in local atomic rearrangements; a stress-block yield when the elastic stresses it is exposed to by the surrounding stress blocks satisfies some yield criteria (e.g., the von Mises yield condition) and after yield the elastic (shear) stresses in the stress block are reduced. It is clear that immediately after the rapid plastic deformations the stress blocks in the plastically deformed volume will be in a ''critical'' state with a distribution of local stresses such that some stress blocks are almost ready to undergo plastic deformation. This implies that thermal processes will be of crucial importance; slow relaxation (creep) will occur and the contact area will increase slowly with time. In this section we develop a general (mean-field) theory of time-dependent plastic deformation in solids that may be used for many applications involving creep and relaxation of stress distributions in disordered solids.

The local yield processes described above may involve very small volume elements (stress blocks) with a diameter ~10–100 Å. Such small yield events cannot easily be detected directly in plastic deformation under most practical conditions, e.g., during the elongation of a macroscopic solid bar. (It might, however, be possible to probe the yield events indirectly by registering the elastic waves in a solid block during slow plastic deformation. Associated with each yield event should be an emitted elastic wave pulse, which may be registered by a sound detector with high time resolution.) However, discrete yield events have been detected in nanoindentation experiments. Figure 1 shows the result of an experiment where a diamond indenter with a blunt end (radius of curvature of approximately 2050 Å) is pushed against a gold (110) surface.[9] Note the series of yield events separated by elastic loading. If the unloading occurs before the first yield event no hysteresis is observed as expected when only elastic deformation occurs. Thus the Au surface deforms elastically between each yield event. We also note that the observed yield stress (~5 GPa) in these nanoscale experiments is much higher than the macroscopic yield stress of gold (about 1 MPa for a single crystal of gold), i.e., the yield stress on the nanoscale is much higher than on macroscopic length scales. The reason for this is discussed in, e.g., Ref. 2.

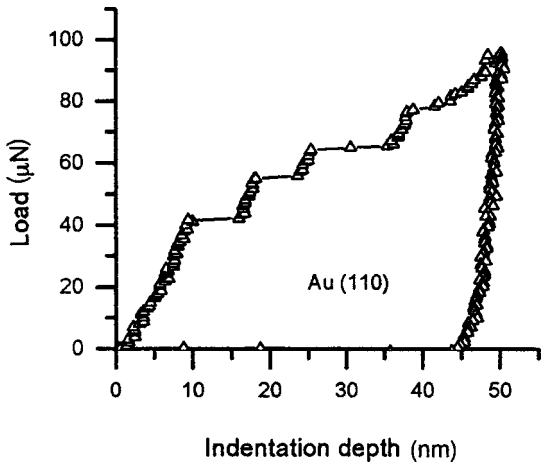

FIG. 1. Load-displacement curve for Au single crystal. From Ref. 9.

It has been found experimentally that plastic deformation and creep only depend on the shear stresses and that the volume of the body does not change during plastic deformation or creep. Thus, if we introduce the hydrostatic pressure $p=-\sigma_{kk}/3$, then plastic deformation does not depend on p but only on the stress deviator

$$s_{ij}=\sigma_{ij}+p\,\delta_{ij}.$$

Note that $s_{ii}=0$. Similarly, if ε_{ij} denotes the strain tensor, the strain deviator is defined by

$$e_{ij}=\varepsilon_{ij}-\delta_{ij}\varepsilon_{kk}/3.$$

When only elastic deformation occurs

$$e_{ij}=s_{ij}(1+\nu)/E,$$

where E is the elastic modulus and ν the Poisson ratio. Since the onset of plastic yielding does not depend on p the yield condition is a function only of s_{ij}. Since $s_{ii}=0$, the simplest nonzero invariant (under rotations) that can be formed from s_{ij} is $s_{ij}s_{ij}$. In the theory of von Mises,[10] which has been

found to be in very good agreement with experiments, the plastic yield criteria is taken to be $s_{ij}s_{ij}=s_0^2$, where s_0 is a constant that can be related to the yield stress σ_a during uniaxial tension, where the stress tensor and the stress deviator have the form

$$\sigma_{ij}=\begin{pmatrix}\sigma & 0 & 0\\ 0 & 0 & 0\\ 0 & 0 & 0\end{pmatrix},\quad s_{ij}=\begin{pmatrix}2\sigma/3 & 0 & 0\\ 0 & -\sigma/3 & 0\\ 0 & 0 & -\sigma/3\end{pmatrix}.$$

Thus $s_{ij}s_{ij}=2\sigma^2/3$ so that $2\sigma_a^2/3=s_0^2$. The von Mises yield criteria can be expressed as follows: A body flows plastically if the elastic energy per unit volume due to shear deformations reaches a critical value. This result is trivial to prove if one note that the elastic energy per unit volume is given by

$$\frac{dU}{dV}=\tfrac{1}{2}\,\sigma_{ij}\varepsilon_{ij}=\tfrac{1}{2}\,(s_{ij}-p\,\delta_{ij})(e_{ij}+\delta_{ij}\varepsilon_{kk}/3)$$
$$=\tfrac{1}{2}\,s_{ij}e_{ij}-\tfrac{1}{2}\,p\varepsilon_{kk}.$$

Since ε_{kk} is the increase in the volume per unit volume due to the elastic deformations, the last term in the expression above is the elastic energy due to the volume change, while the first term is the elastic energy due to the shear deformations only, and can be written as

$$\frac{dU_1}{dV}=\frac{1+\nu}{2E}\,s_{ij}s_{ij},$$

Thus plastic flow occurs when $dU_1/dV=(1+\nu)\sigma_a^2/3E$.

Let us now introduce the stress (probability) distribution function $P(s_{ij},t)$, which satisfies

$$\frac{dP}{dt}=\frac{\partial P}{\partial t}+\frac{\partial P}{\partial s_{ij}}\dot{s}_{ij}=-\nu_0 e^{-\beta\Delta E(s_{ij})}P+\dot{N}\delta(s_{ij}),\qquad(1)$$

where $P=0$ if $s_{ij}s_{ij}>s_0^2$, and

$$\delta(s_{ij})=\delta(s_{11})\,\delta(s_{12})\cdots\delta(s_{33}),$$

and where $\dot{N}$ is determined so that probability is conserved, i.e.,

$$\int d^9s\,P(s_{ij},t)=1,\qquad(2)$$

where $d^9s=ds_{11}ds_{12}\cdots ds_{33}$ is a volume element in the nine-dimensional s space and where the integral is over the region $s_{ij}s_{ij}\leqslant s_0^2$. In Eq. (1) we have assumed that after shear melting the shear stress in a stress block is reduced to zero. Integrating Eq. (1) over s space gives

$$\frac{\partial}{\partial t}\int d^9s\,P=-\dot{s}_{ij}\int d^9s\,\frac{\partial P}{\partial s_{ij}}-\nu_0\int d^9s\,e^{-\beta\Delta E(s_{ij})}P+\dot{N}.$$

Using Eq. (2) the lhs of this equation vanishes. Using Gauss theorem we have

$$\int d^9s\,\frac{\partial P}{\partial s_{ij}}=\int_S d^8s\,Pn_{ij},$$

where d^8s is a surface element of the eight-dimensional sphere S determined by $s_{ij}s_{ij}=s_0^2$, and where the unit ''vector'' (in s space) $n_{ij}=s_{ij}/s_0$ is everywhere perpendicular to the surface S. Thus we get

$$\dot{N}=\dot{s}_{ij}\int_S d^8s\,Pn_{ij}+\nu_0\int d^9s\,e^{-\beta\Delta E(s_{ij})}P.\qquad(3)$$

We can interpret the two terms in this equation as the rate at which a stress block shear yields, as a result of (a) being driven over the barrier towards shear yielding by the increase in the elastic stress (first term), or (b) as a result of thermal excitation over the barrier (second term). We can visualize process (b) as occurring when a (thermally excited) elastic wave packet reaches the stress block and locally increases the shear stress $s_{ij}\rightarrow s_{ij}^0$ to the yield condition $s_{ij}^0s_{ij}^0=s_0^2$. Using the elastic continuum model one can estimate the energy barrier $\Delta E(s_{ij})$ as follows. Assume that a stress block has the form of a sphere with the radius R, which may be of order $\sim$100 Å. By applying an external work ΔE on the surface $r=R$ of the stress block it is possible to change the shear stress in the stress block from s_{ij} to s_{ij}^0. Using the theory of elasticity one can calculate (see Appendix A)

$$\Delta E=A(s_{ij}^0-s_{ij})s_{ij}^0,\qquad(4)$$

where

$$A=\frac{5\pi R^3(1-\nu^2)}{E(4-5\nu)}.\qquad(5)$$

The energy barrier $\Delta E(s_{ij})$ in Eq. (1) is obtained by minimizing Eq. (4) with respect to s_{ij}^0 with the constraint that $s_{ij}^0s_{ij}^0=s_0^2$ and $s_{kk}^0=0$. To solve this problem let us form

$$F=A(s_{ij}^0-s_{ij})s_{ij}^0+\alpha(s_{ij}^0s_{ij}^0-s_0^2)+\beta s_{kk}^0,$$

where α and β are Lagrange multipliers. Minimizing F with respect to s_{ij}^0 gives

$$s_{ij}^0=\frac{As_{ij}}{2A+2\alpha}\qquad(6)$$

and from the condition $s_{ij}^0s_{ij}^0=s_0^2$ we get

$$\frac{A}{2A+2\alpha}=\frac{s_0}{(s_{ij}s_{ij})^{1/2}}.\qquad(7)$$

Substituting Eqs. (6) and (7) in Eq. (4) gives

$$\Delta E=As_0^2[1-(s_{ij}s_{ij})^{1/2}/s_0]\equiv\epsilon[1-(s_{ij}s_{ij})^{1/2}/s_0],\quad(8a)$$

where

$$\epsilon=As_0^2=\frac{10\pi R^3(1-\nu^2)\sigma_a^2}{3E(4-5\nu)}.\qquad(8b)$$

Finally, we must specify $\dot{s}_{ij}$ occurring in Eq. (1), which is the rate of increase of the shear stress s_{ij} due to *local elastic deformations of a stress block*, i.e.,

$$\dot{s}_{ij}=\frac{E}{1+\nu}(\dot{e}_{\rm el}^{\rm loc})_{ij}.\qquad(9)$$

We will show below that the local strain deviator rate is simply the sum of the plastic and elastic strain deviator rates, i.e.,

$$(\dot{e}_{\rm el}^{\rm loc})_{ij}=(\dot{e}_{\rm pl})_{ij}+(\dot{e}_{\rm el})_{ij}\equiv\dot{e}_{ij}, \tag{10}$$

where

$$(e_{\rm el})_{ij}=\frac{1+\nu}{E}\langle s_{ij}\rangle, \tag{11}$$

$$\langle s_{ij}\rangle=\int d^9s\, s_{ij}P(s_{kl},t).$$

If we assume that the elastic shear strain $(1+\nu)s_{ij}/E$ in a stress block is completely converted into plastic strain during a shear yield event, then the rate of plastic deformation is

$$(\dot{e}_{\rm pl})_{ij}=\frac{1+\nu}{E}\left(\int_S d^8s\, s_{ij}Pn_{kl}\dot{s}_{kl}+\nu_0\int d^9s\, e^{-\beta\Delta E(s_{kl})}s_{ij}P\right). \tag{12}$$

The two terms in the parentheses on the rhs of this equation are the product of the rate at which a stress block shear yields and the plastic strain gained in such a process [which equals $(1+\nu)s_{ij}/E$]: the first term results from the stress block being driven over the barrier towards shear yield by the increase in the elastic stress, while the second term results from thermal excitation over the barrier $\Delta E(s_{ij})$.

To derive an expression for $\dot{s}_{ij}$, let us multiply Eq. (1) with s_{ij} and integrate over s space:

$$\frac{\partial}{\partial t}\int d^9s\, s_{ij}P=-\int d^9s\, s_{ij}\frac{\partial P}{\partial s_{kl}}\dot{s}_{kl}-\nu_0\int d^9s\, e^{-\beta\Delta E(s_{kl})}s_{ij}P. \tag{13}$$

But

$$\int d^9s\, s_{ij}\frac{\partial P}{\partial s_{kl}}=\int d^9s\,\frac{\partial}{\partial s_{kl}}(s_{ij}P)-\delta_{ik}\delta_{jl}\int d^9s\, P=\int_S d^8s\, s_{ij}Pn_{kl}-\delta_{ik}\delta_{jl}, \tag{14}$$

where we have used Gauss theorem and the normalization condition (2). Substituting Eq. (14) in Eq. (13) gives

$$\frac{\partial}{\partial t}\int d^9s\, s_{ij}P=\dot{s}_{ij}-\int_S d^8s\, s_{ij}Pn_{kl}\dot{s}_{kl}-\nu_0\int d^9s\, e^{-\beta\Delta E(s_{kl})}s_{ij}P. \tag{15}$$

Using Eqs. (11), (12), and (15) gives

$$\dot{s}_{ij}=\frac{E}{1+\nu}[(\dot{e}_{\rm pl})_{ij}+(\dot{e}_{\rm el})_{ij}]=\frac{E}{1+\nu}\dot{e}_{ij}, \tag{16}$$

where $\dot{e}_{ij}$ is the total strain deviator rate. Substituting Eq. (16) in Eq. (1) gives

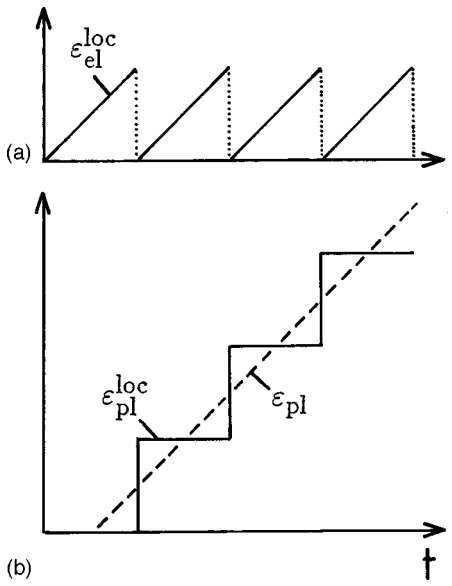

FIG. 2. (a) The local elastic strain in a stress block as a function of time during stationary creep. (b) Solid line, local plastic strain; dashed line, macroscopic plastic strain obtained by averaging the microscopic plastic strain over time.

$$\frac{\partial P}{\partial t}+\frac{E}{1+\nu}\frac{\partial P}{\partial s_{ij}}\dot{e}_{ij}+\nu_0 e^{-\beta\Delta E(s_{ij})}P-\dot{N}\delta(s_{ij})=0. \tag{17}$$

This equation can be solved using the method of characteristic curves. In the next section we consider the simplest (but very important) case of uniaxial tension.

I have proved above that the local elastic strain rate $\dot{e}_{\rm el}^{\rm loc}$ is identical to the total strain rate $\dot{e}$. To close this section, I give some simple physical arguments for why this equation holds. I consider two limiting cases, namely the cases where (a) the elastic strain rate vanishes and (b) the plastic strain rate vanishes. Case (a) prevails during stationary creep (uniaxial tension) where $e_{\rm el}=$const. Consider a stress block during stationary creep. Figure 2(a) shows the local elastic strain at the stress block. The elastic strain increases linearly with time until the shear stress reaches the critical value where local shear yield occur. After shear yield (which is assumed to occurs instantaneously in the present theory), the stress block is in a state where the shear stress and hence the local elastic strain is zero. This cycle repeats itself periodically. Thus, the local plastic shear strain will take the form shown by the solid line in Fig. 2(b). The corresponding macroscopic plastic strain is obtained by averaging the microscopic plastic strain over time and is given by the dashed line in Fig. 2(b). It is clear that $\dot{e}_{\rm pl}$, which is given by the slope of the solid line in Fig. 2(b), is identical to $\dot{e}_{\rm el}^{\rm loc}$, which is given by the slope of the tilted lines in Fig. 2(a). Thus, since the macroscopic elastic strain is constant, it follows that $\dot{e}_{\rm el}=0$ so that $\dot{e}_{\rm el}^{\rm loc}=\dot{e}_{\rm pl}=\dot{e}_{\rm pl}+\dot{e}_{\rm el}=\dot{e}$ and Eq. (10) is valid in this case. Next, let us consider case (b). This case prevail if, e.g., an elastic block is exposed to very weak external forces. In this case there is no plastic deformation so that $\dot{e}_{\rm el}^{\rm loc}=\dot{e}_{\rm el}=\dot{e}$ so that Eq. (10) holds trivially in this limiting case.

III. UNIAXIAL TENSION

For uniaxial tension as in Fig. 3 the strain deviator rate $\dot{e}_{ij}$ has the form

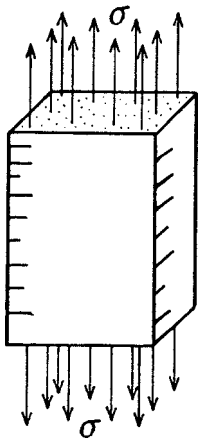

FIG. 3. A solid block under uniaxial tension.

$$\dot{e}_{ij}=\begin{pmatrix} \dot{e} & 0 & 0 \\ 0 & -\dot{e}/2 & 0 \\ 0 & 0 & -\dot{e}/2 \end{pmatrix} \tag{18}$$

and it is then easy to show that Eq. (17) is satisfied with

$$P(s_{ij},t)=\tfrac{3}{2}\,P(\sigma,t)\,\delta(s_{22}+\sigma/3)\,\delta(s_{33}+\sigma/3)\prod_{i\neq j}\delta(s_{ij}), \tag{19}$$

where $\sigma=3s_{11}/2$. Thus $\langle s_{ij}\rangle$ and the stress tensor have the form

$$\langle s_{ij}\rangle=\begin{pmatrix} 2\langle\sigma\rangle/3 & 0 & 0 \\ 0 & -\langle\sigma\rangle/3 & 0 \\ 0 & 0 & -\langle\sigma\rangle/3 \end{pmatrix},$$

$$\langle\sigma_{ij}\rangle=\begin{pmatrix} \langle\sigma\rangle & 0 & 0 \\ 0 & 0 & 0 \\ 0 & 0 & 0 \end{pmatrix}.$$

Substituting Eq. (19) in Eq. (17) gives the following equation for $P(\sigma)$:

$$\frac{\partial P}{\partial t}+\frac{3}{2}\,\frac{E\dot{e}}{1+\nu}\,\frac{\partial P}{\partial\sigma}+\nu_0 e^{-\beta\Delta E(\sigma)}P-\dot{N}\delta(\sigma)=0, \tag{20}$$

where

$$\Delta E(\sigma)=\epsilon(1-|\sigma|/\sigma_a). \tag{21}$$

If we consider a cylindrical block of height $l(t)$ exposed to a surface stress $\sigma(t)$ on the top and bottom surfaces (see Fig. 3), then the strain rate

$$\dot{\varepsilon}_{11}=\dot{l}/l(t)$$

can be related to the strain deviator rate $\dot{e}$ as follows. The elastic strain is given by

$$(\varepsilon_{\rm el})_{ij}=\frac{\langle\sigma\rangle}{E}\begin{pmatrix} 1 & 0 & 0 \\ 0 & -\nu & 0 \\ 0 & 0 & -\nu \end{pmatrix}$$

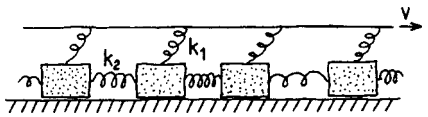

FIG. 4. Spring-block model of uniaxial tension.

so that

$$\varepsilon_{ii}=(1-2\nu)\langle\sigma\rangle/E,$$

where we have used that the plastic deformation occurs without change in the density so that $(\varepsilon_{\rm pl})_{ii}=0$. Thus we get

$$\varepsilon_{ij}=e_{ij}+\delta_{ij}(1-2\nu)\langle\sigma\rangle/3E,$$

or, since $\dot{\varepsilon}_{11}=\dot{l}/l$ and from Eq. (18) $\dot{e}_{11}=\dot{e}$:

$$\dot{l}/l=\dot{e}+\langle\dot{\sigma}\rangle(1-2\nu)/3E.$$

Since $\langle\sigma\rangle=\sigma(t)$ we can write

$$\dot{e}=\dot{l}/l-\dot{\sigma}(1-2\nu)/3E. \tag{22}$$

In particular, for stationary creep, where $\sigma(t)$ is independent of time, $\dot{e}=\dot{l}/l$ is time independent.

IV. BLOCK-SPRING MODEL

The time-dependent deformation of a solid bar under uniaxial tension (Fig. 3) can be (approximately) mapped onto the one-dimensional spring-block model shown in Fig. 4. The blocks in the figure correspond to the stress blocks in the solid bar. Thus the linear size of a block is of order $D\sim R$ and the mass of a block $m\sim\rho D^3$. A block is pinned until the stress at the interface reaches a critical value σ_a (corresponding to the static friction force), at which point the block starts to slip. The slip corresponds to the plastic deformation of a stress block in the solid bar. After the rapid slip the block will stick, which corresponds to ''refreezing'' of the stress block. We will show below that the springs k_1 and k_2 are determined by the elastic properties of the solid bar, and that the driving velocity v (which may vary with time) is proportional to the strain rate.

I have shown that,[5] in the mean-field approximation, the interfacial stress distribution $P(\sigma,t)$ in the model in Fig. 4 satisfies

$$\frac{\partial P}{\partial t}+\frac{k_1 v}{D^2}\,\frac{\partial P}{\partial\sigma}+\overline{\nu}_0 e^{-\beta\Delta E(\sigma)}P-\dot{N}\delta(\sigma)=0, \tag{23}$$

where

$$\Delta E=\overline{\epsilon}[1-(\sigma/\sigma_a)^2], \tag{24}$$

with

$$\overline{\epsilon}=\frac{(D^2\sigma_a)^2}{2(k_1+2k_2)}. \tag{25}$$

Now, Eq. (23) has the same general form as Eq. (20) and if we define

$$v=D\dot{e}, \tag{26}$$

then Eq. (20) and Eq. (23) are formally identical if we identify

$$\frac{k_1 D\dot{e}}{D^2}=\frac{3}{2}\frac{E\dot{e}}{1+\nu}, \tag{27}$$

or

$$k_1=\frac{3}{2}\frac{DE}{1+\nu}. \tag{28}$$

In addition, we must take

$$\overline{\nu_0}=\nu_0. \tag{29}$$

The activation energy ΔE for the spring-block model differs, however, from that associated with plastic deformation [compare Eq. (21) with Eq. (24)]. However, this difference is not of major importance in most cases since thermal excitation over the barrier ΔE will in most cases be important only when $\sigma\approx\sigma_a$ and in this case we can approximate

$$1-(\sigma/\sigma_a)^2=(1+\sigma/\sigma_a)(1-\sigma/\sigma_a)\approx 2(1-|\sigma|/\sigma_a)$$

so that

$$\epsilon\approx 2\overline{\epsilon}$$

Using Eq. (8b) and Eq. (25) this equation gives

$$\frac{(D^2\sigma_a)^2}{k_1+2k_2}=\frac{5\pi R^3(1-\nu^2)}{E(4-5\nu)}\frac{2\sigma_a^2}{3} \tag{30}$$

or

$$\frac{(D/R)^3}{1+2k_2/k_1}=\frac{5\pi(1-\nu)}{4-5\nu}. \tag{31}$$

Since from general argument (see Ref. 5) $k_1\approx k_2$ and if $\nu\approx 0.5$ (typical for metals) we get $D\approx 2.5R$, which is consistent with the interpretation of the blocks in Fig. 4 as the stress blocks in the solid in Fig. 3.

In order to calculate the dynamical behavior of the spring-block model in Fig. 4, I have used a similar procedure as in Ref. 5. That is, a block starts to slide when the spring force acting on it reaches a critical value (the pinning force) $F_a=\sigma_a D^2$, either as a result of the increase of the pulling (spring) force, or else due to a thermal fluctuation. The thermal excitation over the pinning barrier is assumed to occur in a stochastic (random) manner and is determined using random numbers as described in Ref. 5. During sliding the block experiences a kinetic friction force, $-m\gamma\dot{x}_i$, which is proportional to the sliding velocity. In Ref. 5 we assumed that a sliding block returns to the pinned state when the sliding velocity vanishes at the end of a rapid local slip process. In the present study I have used another criterion: I assume that if the magnitude $v_i=|\dot{x}_i|$ of the velocity of a sliding block is below some given (small) critical velocity v_c, the motion of the block *may* abruptly stop. More exactly, if $p=[v_c-v_i(t)]/v_c$ (note: $0<p<1$), then if $Cr<p$, where r is a random number uniformly distributed in the interval $[0,1]$ and where C is a fixed number, the block will stop to move during the short time interval $[t,t+\Delta]$ (where Δ is the time step used in integrating the equation of motion for the blocks). This criterion has been chosen for reasons which are not obviously relevant in the present context, but which turn out to give results virtually indistinguishable from those which follow using the other criteria presented above and used earlier in Ref. 5.

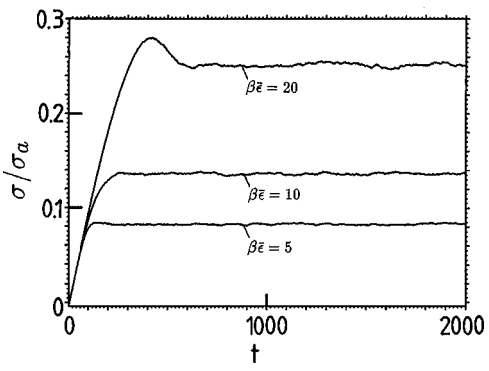

FIG. 5. The dependence of the force (or stress) on time for a few different temperatures corresponding to $\beta\epsilon=5$, 10, and 20. In each case the system starts from a relaxed configuration nearly without internal stress (i.e., the blocks in Fig. 4 are nearly uniformly distributed). The drive velocity $v=0.001$ and $k_1=k_2=1$.

In what follows, we use dimensionless variables, measuring time in units of $(m/k_1)^{1/2}$, distance in units of F_a/k_1, and force in units of F_a. In all the numerical results presented below we have, unless otherwise stated, used $k_1=k_2=1$, $C=0.1/\Delta$ (with $\Delta=0.005$), $v_c=0.02$, $\gamma=1$, and $\overline{\nu}=0.1$.

We now present some numerical results to illustrate the consequences of the spring-block model of uniaxial plastic deformation (see also Ref. 5). Figure 5 shows the relation between the stress and time when the drive speed $v=0.001$, and where we have started with a nearly fully relaxed (annealed) state (the distribution of blocks at $t=0$ was nearly uniform: the fluctuation away from the perfect uniform state was only 1%). We show results for three different temperatures corresponding to $\beta\overline{\epsilon}=5$, 10, and 20. At the lowest temperature ($\beta\overline{\epsilon}=20$) one observes a nearly linear rise of the stress at short times, until the ''upper yield stress'' (the maximum stress) has been reached, followed by continuous plastic flow. At lower temperatures (for steel one typically has $\epsilon=1-2$ eV, and since $k_BT\approx 0.025$ meV at room temperature one typically has $\beta\epsilon=40-80$) the upper yield stress is larger as illustrated in Fig. 6 for $\beta\overline{\epsilon}=40$. At ''high'' temperatures ($\beta\overline{\epsilon}=5$ and 10) the dynamics is more liquidlike although even in these cases there is a nearly linear initial increase in the stress at short times because of elastic deformation.

V. STATIONARY CREEP

Assume that a rectangular solid block is exposed to a constant surface stress σ_0 on two opposite surfaces as indicated in Fig. 3. If $l(t)$ denote the length of the block at time t and $\varepsilon_{11}=\varepsilon$ then

$$\dot{\varepsilon}=\dot{l}/l(t).$$

After an initial relaxation time period τ, during which the stress distribution $P(s_{ij},t)$ changes from the initial $t=0$ form (which is determined by the previous history of defor-

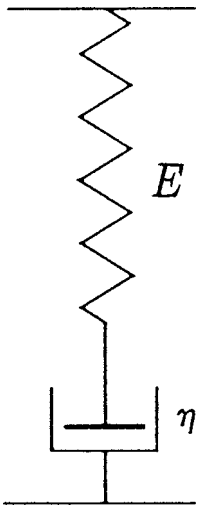

FIG. 6. Rheological model of the linear stress-strain response of a solid block.

mations the block has been exposed to) to its steady state form, we expect $\dot{\varepsilon}$ to depend only on σ_0. Thus

$$\dot{\varepsilon}=\dot{e}=f(\sigma_0)$$

so that

$$l(t)=l(0)e^{f(\sigma_0)t}.$$

Note that we have assumed that σ_0 is constant, and since the area $A(t)$ depends on time in such a way that the volume $V=A(t)l(t)$ is constant (plastic deformations usually occur without any change in the volume of the body), it follows that the total force that acts on the surface A decreases with time.

We now determine the function $f(\sigma_0)$. In the present case $P(\sigma)$ is time independent and $\dot{e}=\dot{\varepsilon}$ so that

$$\frac{E\dot{\varepsilon}}{1+\nu}\frac{\partial P}{\partial\sigma}+\frac{2\nu_0}{3}e^{-\beta\Delta E(\sigma)}P-\dot{N}\delta(\sigma)=0, \tag{32}$$

where

$$\Delta E(\sigma)=\epsilon[1-\sigma/\sigma_a]$$

for $\sigma\geqslant 0$. The general solution to Eq. (32) is

$$P=C\exp\Bigg(-[2\nu_0(1+\nu)/3E\dot{\varepsilon}]\int_0^{\sigma}d\sigma' \times\exp[-\beta\epsilon(1-\sigma'/\sigma_a)]\Bigg) \tag{33}$$

for $0\leqslant\sigma<\sigma_a$ and zero otherwise. Let us introduce $\alpha=2\nu_0(1+\nu)\sigma_a/(3E\dot{\varepsilon}\beta\epsilon)$ so that

$$P=C\exp\Bigg(-\beta\epsilon\alpha\int_0^{\sigma/\sigma_a}dx\exp[-\beta\epsilon(1-x)]\Bigg). \tag{34}$$

Thus the average stress

$$\langle\sigma\rangle=\sigma_0=\int_{-\sigma_a}^{\sigma_a}d\sigma\,\sigma P(\sigma), \tag{35}$$

in units of σ_a, depends only on the two parameters α and $\beta\epsilon$. Let us first consider the high-strain-rate limit where $\alpha\ll 1$. In this case Eq. (34) can be expanded to leading order in α and substituting the result in Eq. (35) gives to leading order in $1/\dot{\varepsilon}$ (see Appendix B):

$$\langle\sigma\rangle=\frac{\sigma_a}{2}\left(1-\frac{\alpha}{\beta\epsilon}\right)=\frac{\sigma_a}{2}\left(1-\frac{2\nu_0(1+\nu)\sigma_a}{3E\dot{\varepsilon}(\beta\epsilon)^2}\right). \tag{36}$$

Thus, at high strain rate the stress approaches the limiting value $\sigma_a/2$. We note, however, that this limiting value results from the assumption that after shear yield the stress in a stress block vanishes.

Next, let us consider the small $\dot{\varepsilon}$ limit where $\alpha\gg 1$ but assume $\alpha\exp(-\beta\epsilon)\ll 1$. In this case we show in Appendix B that

$$\langle\sigma\rangle=\frac{\sigma_a}{2}\left(1-\frac{1}{\beta\epsilon}\ln\alpha\right)=\frac{\sigma_a}{2}\left[1+\frac{1}{\beta\epsilon}\ln\left(\frac{3E\dot{\varepsilon}\beta\epsilon}{2\nu_0(1+\nu)\sigma_a}\right)\right]. \tag{37}$$

Thus, in this extremely important limiting case, the stress is proportional to the logarithm of the strain rate. This relation is valid for most ''normal'' solids under typical temperatures (see Sec. XI). A similar relation between σ and $\dot{\varepsilon}$ can be derived using simpler, but less rigorous, arguments due to Eyring, involving stress-biased thermal excitation over pinning barriers.

In the extreme small $\dot{\varepsilon}$ limit where $\alpha\gg 1$ and $\alpha\exp(-\beta\epsilon)\gg 1$ we get (see Appendix B)

$$\langle\sigma\rangle=\frac{\sigma_a}{\alpha\beta\epsilon}e^{\beta\epsilon}=\frac{3E\dot{\varepsilon}}{2\nu_0(1+\nu)}e^{\beta\epsilon}=\eta\dot{\varepsilon}, \tag{38}$$

where the *viscosity*

$$\eta=\frac{3E}{2\nu_0(1+\nu)}e^{\beta\epsilon}. \tag{39}$$

This equation is valid at high enough temperature (or low enough shear rate) and shows that the strain rate is proportional to the applied stress. Thus, at high temperature the model exhibit *Newtonian flow*, as is characteristic of liquids.

VI. LINEAR RESPONSE TO OSCILLATORY STRAIN

We consider the response of a solid bar (Fig. 3) to an oscillatory strain. Let us write

$$e(t)=\int d\omega\tilde{e}(\omega)e^{-i\omega t},$$

$$\tilde{e}(\omega)=\frac{1}{2\pi}\int dt e(t)e^{i\omega t}.$$

Assume that the amplitude $\dot{e}(t)$ is so small that we can calculate the stress $\langle\sigma\rangle$ to linear order in $\dot{e}$. We write $P=P_0+P_1$, where P_0 and P_1 are of zero and first order in $\dot{e}$, respectively. Substituting $P=P_0+P_1$ in Eq. (20) gives to zero order in $\dot{e}$ (for $\sigma\neq 0$):

$$\frac{\partial P_0}{\partial t}+\nu_0 e^{-\beta\Delta E(\sigma)}P_0=0$$

with the (steady state) solution

$$P_0=\delta(\sigma).$$

Next, to linear order in $\dot{e}$ we get for $\sigma\neq 0$:

$$\frac{\partial P_1}{\partial t}+\frac{3}{2}\frac{E\dot{e}}{1+\nu}\frac{\partial P_0}{\partial \sigma}+\nu_0 e^{-\beta\Delta E(\sigma)}P_1=0 \tag{40}$$

or

$$(-i\omega)\tilde{P}_1+\frac{3}{2}\frac{E}{1+\nu}(-i\omega\tilde{e})\delta'(\sigma)+\nu_0 e^{-\beta\Delta E(\sigma)}\tilde{P}_1=0 \tag{41}$$

so that

$$\tilde{P}_1=\frac{3}{2}\frac{E}{(1+\nu)}\frac{(-i\omega\tilde{e})\delta'(\sigma)}{(i\omega-\nu_0 e^{-\beta\Delta E(0)})}.$$

Thus

$$\int d\sigma(P_0+P_1)=\int d\sigma\, P_0=1,$$

while

$$\langle\tilde{\sigma}\rangle=\int d\sigma\,\sigma\tilde{P}=\int d\sigma\,\sigma\tilde{P}_1=-\frac{3}{2}\frac{E}{(1+\nu)}\frac{(-i\omega\tilde{e})}{(i\omega-\nu_0 e^{-\beta\epsilon})}.$$

This equation is equivalent to

$$\frac{d\langle\sigma\rangle}{dt}-\frac{3}{2}\frac{E\dot{e}}{1+\nu}+\nu_0 e^{-\beta\epsilon}\langle\sigma\rangle=0. \tag{42}$$

Let us for simplicity denote $\langle\sigma\rangle=\sigma$. Combining Eq. (42) with Eq. (22) (with $\dot{\varepsilon}=\dot{l}/l$), gives

$$\dot{\varepsilon}=\dot{\sigma}/E+\sigma/\eta, \tag{43}$$

where the viscosity η is defined by Eq. (39). When $\dot{\sigma}=0$ then Eq. (43) reduces to Eq. (38). Note that Eq. (43) is the standard formula for the linear response of glassy solids (see, e.g., Ref. 10), usually described by a rheological model of the form indicated in Fig. 6; it is gratifying that this result follows from the theory.

The study presented above can be easily generalized to obtain the linear response relation between the strain and stress in a general triaxial case. Using Eq. (17) and following the same procedure as above gives

$$\dot{e}_{ij}=\frac{1+\nu}{E}\frac{d\langle s_{ij}\rangle}{dt}+\frac{3}{2\eta}\langle s_{ij}\rangle.$$

Since the plastic deformation is assumed to occur without volume change we have as before

$$\langle\sigma_{ii}\rangle=\frac{E}{1-2\nu}\varepsilon_{ii}.$$

These are the standard linear response tensor relations between stress and strain in a linear viscoelastic media.

In the special case of uniaxial tension with

$$\varepsilon=\varepsilon_0\sin(\omega t)$$

it is easy to calculate [using Eq. (43)] the energy dissipation per unit volume and unit time

$$\frac{\Delta E}{VT}=\tfrac{1}{2}E\varepsilon_0^2\frac{(\omega\tau)^2}{(\omega\tau)^2+1}(1/\tau),$$

where the relaxation time $\tau=\eta/E$.

VII. NONLINEAR RESPONSE TO OSCILLATORY STRAIN

In this section I present numerical results for the nonlinear relation between the stress and an oscillatory strain. We make use of the (approximate) equivalence between the (mean-field) equation of motion for the spring-block system, and the uniaxial tension of a solid block (see Sec. IV). It may, however, be possible to solve Eq. (20) analytically even in the nonlinear regime (see Appendix C), but I have not yet been able to obtain an analytical solution in closed form for the relation between $\langle\sigma\rangle$ and $\varepsilon(t)$.

Let us write the driving displacement and velocity as

$$x(t)=x_0\sin(\omega t),$$

$$v(t)=x_0\omega\cos(\omega t).$$

In the linear response limit one obtain from Eq. (23) [compare with Eq. (42)]:

$$\frac{d\langle\sigma\rangle}{dt}-\frac{k_1 v}{D^2}+\overline{\nu}_0 e^{-\beta\epsilon}\langle\sigma\rangle=0.$$

If N denote the number of blocks then the force $F=ND^2\langle\sigma\rangle$ satisfies

$$\dot{F}+\overline{\nu}_0 e^{-\beta\epsilon}F=Nk_1 v. \tag{44}$$

For ''large'' x_0 the relation between F and $x(t)$ will be nonlinear. However, it is clear that independent of the initial stress distribution, $P(\sigma,0)$, after a long enough time $P(\sigma,t)$ will be a periodic function of time with the period $T=2\pi/\omega$. This implies that for large times $F(t)$ will be of the general form

$$F(t)=\frac{1}{2i}\sum_n (F_n e^{in\omega t}-\text{c.c.}), \tag{45}$$

where

$$F_n=\frac{2i}{T}\int_0^T dt\,F(t)e^{-in\omega t}. \tag{46}$$

It is clear that $P(\sigma,t)=P(-\sigma,T/2+t)$, which implies that $F_n=0$ for even n. We define the impedance

$$Z=F_1/x_0.$$

In the linear response case F is determined by Eq. (44) so that in this case $F_n=0$ for $n\neq 1$, while

$$F_1=Nk_1x_0\frac{i\omega\tau}{1-i\omega\tau},$$

where the relaxation time

$$\tau = e^{\beta\epsilon}/\overline{\nu}_0 .$$

Thus

$$Z = Nk_1 \frac{i\omega\tau}{1 - i\omega\tau}$$

so that

$$\mathrm{Re}\, Z = Nk_1 \frac{(\omega\tau)^2}{1+(\omega\tau)^2}, \quad \mathrm{Im}\, Z = Nk_1 \frac{\omega\tau}{1+(\omega\tau)^2}. \quad (47)$$

When $\omega\tau \gg 1$ these formulas reduce to $\mathrm{Re}\, Z = Nk_1$ and $\mathrm{Im}\, Z = Nk_1/\omega\tau$. Thus in this limit the real and imaginary part of Z describe the elastic and viscous properties of the system. Let us *define* $\mathrm{Re}\, Z = Nk_{\mathrm{eff}}$ and $\mathrm{Im}\, Z = Nk_1/\omega\tau_{\mathrm{eff}}$ where the effective spring constant $k_{\mathrm{eff}}(x_0,\omega)$ and effective relaxation time $\tau_{\mathrm{eff}}(x_0,\omega)$ in general will depend on the oscillation amplitude x_0 and the oscillation frequency ω.

The dissipated energy takes the form

$$\frac{\Delta E}{T} = \frac{1}{T}\int_0^T dt\, Fv = \tfrac{1}{2}\,\omega x_0\, \mathrm{Im}\, F_1 = \tfrac{1}{2}\,\omega x_0^2\, \mathrm{Im}\, Z$$

$$= \tfrac{1}{2}\, Nk_1 x_0^2/\tau_{\mathrm{eff}}, \quad (48)$$

i.e., the dissipated energy is determined by the fundamental $n=1$ mode, and does not depend on the higher harmonic components. In the linear response limit, Eq. (47) and Eq. (48) gives the (average) energy dissipation per unit time and per block

$$\frac{\Delta E}{NT} = \tfrac{1}{2}\, k_1 x_0^2 \frac{(\omega\tau)^2}{1+(\omega\tau)^2}(1/\tau).$$

Let us now study Z as a function of the amplitude x_0. Figure 7 shows k_{eff} and $1/\tau_{\mathrm{eff}}$ as a function of x_0/x_a where x_a is the displacement necessary in order to increase the local stress at a block from zero to the yield stress σ_a. We show results for $\beta\overline{\epsilon} = 10$ (solid curves) and 20 (dashed curves) with $\overline{\nu}_0 = 0.1$ and the oscillator frequency $\omega = 0.083$. Note that $k_{\mathrm{eff}} \approx k_1$ for $x_0 < 0.3x_a$ when $\beta\overline{\epsilon} = 10$ and for $x_0 < 0.4x_a$ when $\beta\overline{\epsilon} = 20$. It is also interesting to note that in the present case $\mathrm{Im}\, Z$ is maximal at $x_0 \approx 0.5x_a$, rather than at $x_0 = x_a$. Since the energy ''dissipation'' is proportional to $\mathrm{Im}\, Z \sim 1/\tau_{\mathrm{eff}}$ this quantity must be positive for all oscillation amplitudes [see Fig. 7(b)]. However, so such condition exists for $\mathrm{Re}\, Z$, which can take on both positive and negative values [see Fig. 7(a)]. Figure 8 shows the ratios $\mathrm{Im}\, F_3/\mathrm{Im}\, F_1$ and $\mathrm{Re}\, F_3/\mathrm{Re}\, F_1$, as a function of the oscillation amplitude x_0 for $\omega = 0.083$. Note that the harmonic component completely dominates for $x_0 < 0.4x_a$, but for $x_0 > 0.5x_a$ the $n=3$ anharmonic contribution is of similar magnitude as the fundamental $n=1$ contribution. Nevertheless, as stated above, the energy dissipation is determined only by the fundamental ($n=1$) mode even for large oscillation amplitude. It is interesting to note that linear response theory [Eq. (47)] predicts in the present case $k_{\mathrm{eff}} \approx k_1$, while $1/\tau_{\mathrm{eff}} \approx 4.5\times 10^{-6}$ and 2.1×10^{-10} for $\beta\epsilon = 10$ and 20, respectively. These values for $1/\tau_{\mathrm{eff}}$ are much smaller than obtained in the numerical calculations even for x/x_a as small as 0.05. It is clear that the *linear response result for the damping is only valid at extremely small values of* x_0/x_a.

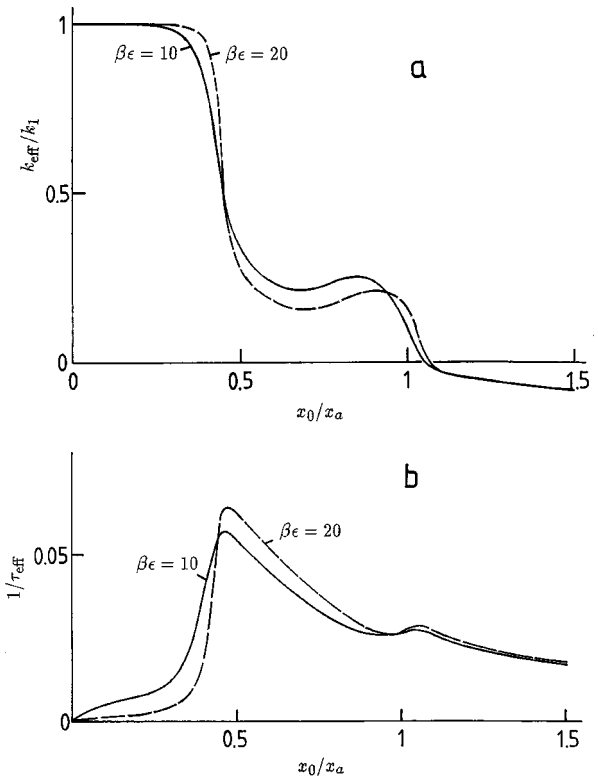

FIG. 7. The dependence of (a) k_{eff} and (b) $1/\tau_{\mathrm{eff}}$ on the oscillation amplitude x_0 in units of the displacement x_a necessary for local shear melting. Results are presented for $\beta\epsilon = 10$ (solid lines) and 20 (dashed lines). For the oscillation frequency $\omega = 0.083$.

We note that the results presented above are only valid for such low frequencies ω that the time it takes for a sound wave to propagate from one side of the solid block to the other side is small compared to $1/\omega$. Since the frequency ω used in the numerical results presented above is very high this requires in general very thin solid blocks (thickness d) in order for the condition $\omega d \ll c$ (where c is the longitudinal sound velocity) to be satisfied. Computer simulations for smaller, but more interesting, frequencies are very time consuming and it would clearly be very useful if one could derive analytical results for $Z(x_0,\omega)$ which cover all cases of interest (see Appendix C).

VIII. RELAXATION AND RECOVERY

In this section we present a short study of relaxation and recovery in the uniaxial deformation of a solid bar. The dis-

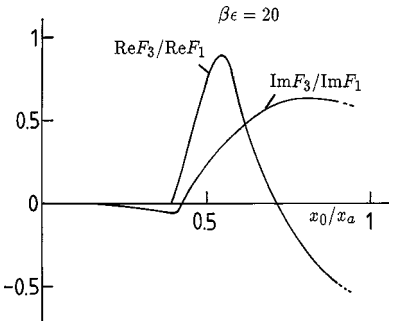

FIG. 8. The ratio $\mathrm{Re}\, F_3/\mathrm{Re}\, F_1$ and $\mathrm{Im}\, F_3/\mathrm{Im}\, F_1$ as a function of the oscillation amplitude x_0. For the oscillation frequency $\omega = 0.083$ and $\beta\epsilon = 20$.

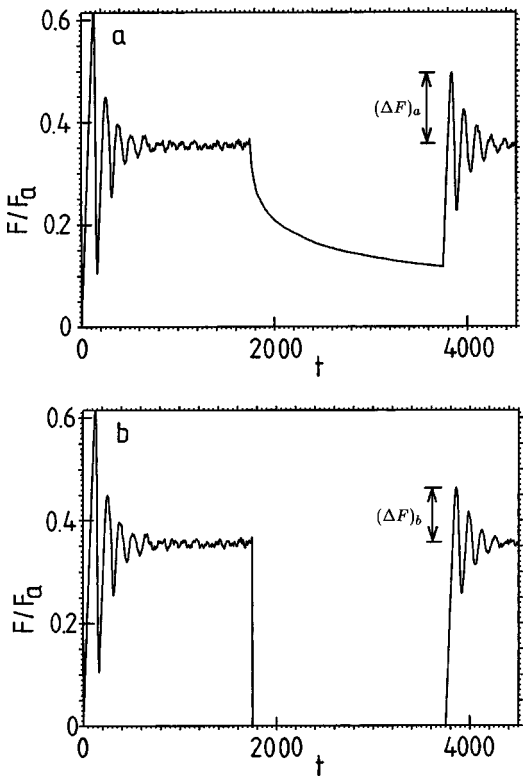

FIG. 9. Stop and start simulations. In case (a) the coordinate x of the drive is fixed ($v=0$) between $t=1750$ and 3750 after which the drive continues with the same velocity $v=0.005$ as before the stop. (b) The same as (a) except that during ''stop'' the coordinate x is rapidly changed until the pulling force vanishes.

cussion is again based on the spring-block model of the plastic deformation process. We consider the following two stop-and-start ''experiments,'' which we refer to as (a) ''stressed aging'' and (b) ''free aging:'' Initially the spring-block system is pulled with a small constant velocity v. At time $t=t_0$ we suddenly stop pulling and in case (a) we keep the coordinate x of the drive fixed ($v=0$) until $t=t_1>t_0$ where we continue to pull with the same velocity v as before the stop. This will give rise to a ''striction'' spike of height $(\Delta F)_a$. In the second ''experiment'' (b) we again stop the motion at $t=t_0$ but instead of keeping x fixed, we rapidly change x until the pulling force vanishes. Again, at time $t=t_1$ we start to pull with the same velocity as before the stop. This will give rise to a ''striction'' spike of height $(\Delta F)_b$. Figures 9(a) and 9(b) show the result of the simulations for the case when $v=0.005$, $\beta\epsilon=40$ and $t_1-t_0=2000$. Note that $(\Delta F)_a>(\Delta F)_b$. Figure 10 shows the ratio $(\Delta F)_a/(\Delta F)_b$ as a function of $\beta\epsilon$ for $v=0.01$. For $\beta\epsilon<28$, $(\Delta F)_a/(\Delta F)_b\approx 1$ but for larger $\beta\epsilon$ the striction-spike (usually referred to as the ''upper yield stress'') is larger for ''stressed aging'' than for ''free aging.'' Striction spikes of the type shown in Fig. 9 have been observed during uniaxial tension experiments, but are usually associated with the motion of impurity atoms, which tend to accumulate in the stress field of dislocations, resulting in a contribution to the pinning of the dislocations. However, the present calculations show that even in the absence of such effects, one expects striction spikes with a ''height'' which depend on the ''stop'' time, the temperature, and on whether the system

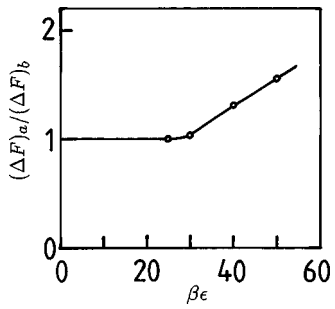

FIG. 10. The ratio $(\Delta F)_a/(\Delta F)_b$ as a function of $\beta\epsilon$ for $v=0.01$.

undergoes ''stressed aging'' or ''free aging.'' Similar effects as described above have also been observed in friction experiments, see Sec. XI C.

IX. MATHEMATICAL DEVELOPMENT AND ILLUSTRATIONS

We consider first the following general problem. Assume that the strain deviator has the form

$$\dot{e}_{ij}=\dot{e}(\mathbf{x},t)M_{ij}(\mathbf{x}), \tag{49}$$

where M_{ij} may depend on the spatial coordinate $\mathbf{x}$ but is independent of time. Without loss of generality we may assume

$$M_{ij}M_{ij}=1, \tag{50}$$

We will now prove that in this case the stress probability distribution function takes the form

$$P(s_{ij},t)=\int ds\ \delta(s_{ij}-sM_{ij})P(s,t) \tag{51}$$

so that, e.g.,

$$\langle s_{ij}\rangle=M_{ij}\int ds\ sP(s,t)=M_{ij}\langle s\rangle. \tag{52}$$

As before we use the definition

$$\delta(s_{ij}-sM_{ij})=\delta(s_{11}-sM_{11})\delta(s_{12}-sM_{12})\cdots\delta(s_{33}-sM_{33}).$$

Now, let us write

$$\delta(s_{ij})=\int ds\ \delta(s_{ij}-sM_{ij})\delta(s). \tag{53}$$

Substituting Eq. (51) and Eq. (53) in Eq. (17) and using that

$$-\frac{\partial}{\partial s}\delta(s_{ij}-sM_{ij})=M_{kl}\frac{\partial}{\partial s_{kl}}\delta(s_{ij}-sM_{ij})$$

and that

$$e^{-\beta\Delta E(s_{ij})}\delta(s_{ij}-sM_{ij})=e^{-\beta\Delta E(sM_{ij})}\delta(s_{ij}-sM_{ij})$$
$$=e^{-\beta\Delta E(s)}\delta(s_{ij}-sM_{ij}),$$

where we have defined

$$\Delta E(s)=\epsilon(1-|s|/s_0),$$

gives

$$\int ds\ \delta(s_{ij}-sM_{ij})\frac{\partial P(s,t)}{\partial t}+\frac{E\dot{e}}{1+\nu}\times\int ds\left[-\frac{\partial}{\partial s}\delta(s_{ij}-sM_{ij})\right]P(s,t)+\int ds\ \delta(s_{ij}-sM_{ij})e^{-\beta\Delta E(s)}P(s,t)=\dot{N}\int ds\ \delta(s_{ij}-sM_{ij})\delta(s). \tag{54}$$

In the second term we perform a partial integration:

$$\int ds\left[-\frac{\partial}{\partial s}\delta(s_{ij}-sM_{ij})\right]P(s,t)=\int ds\ \delta(s_{ij}-sM_{ij})\frac{\partial P(s,t)}{\partial s}. \tag{55}$$

Substituting Eq. (55) in Eq. (54) gives the following equation for $P(s,t)$:

$$\frac{\partial P(s,t)}{\partial t}+\frac{E\dot{e}}{1+\nu}\frac{\partial P(s,t)}{\partial s}+e^{-\beta\Delta E(s)}P(s,t)=\dot{N}\delta(s). \tag{56a}$$

Note also that from Eq. (2) and Eq. (51) it follows that

$$\int_{-s_0}^{s_0} ds\ P(s,t)=1 \tag{56b}$$

so that we can interpret $P(s,t)$ as a probability distribution. If we define

$$\varphi=\frac{E}{1+\nu}\int_0^t dt'\dot{e}(t')=\frac{E}{1+\nu}[e(t)-e(0)],$$

then the formal solution to Eq. (56) can be written as

$$P(s,t)=f[s-\varphi(t)]\exp\left(-\nu_0\int_0^t dt'\ \exp\{-\beta\epsilon[1-|s-\varphi(t)+\varphi(t')|/s_0]\}\right)+\frac{1}{s_0}\left[\exp\left(\int_0^t dt'G(t')\delta[s-\varphi(t)+\varphi(t')]\right)-1\right]\exp\left(-\nu_0\int_0^t dt'\times\exp\{-\beta\epsilon[1-|s-\varphi(t)+\varphi(t')|/s_0]\}\right),$$

where $f(s)=P(s,0)$ is determined by the initial stress distribution function, and where the ''source function'' $G(t)$ must be determined so that condition (56b) is satisfied for all times.

We consider now two applications of the formalism developed above. Let us first show how Eq. (20) results from the present approach. Note first that Eq. (18) can be written as

$$\dot{e}_{ij}=[\dot{e}(\tfrac{3}{2})^{1/2}]M_{ij},$$

where

$$M_{ij}=(\tfrac{2}{3})^{1/2}\begin{pmatrix}1&0&0\\0&-\frac{1}{2}&0\\0&0&-\frac{1}{2}\end{pmatrix},$$

with $M_{ij}M_{ij}=1$. Thus in this case Eq. (56) takes the form

$$\frac{\partial P(s,t)}{\partial t}+\left(\frac{3}{2}\right)^{1/2}\frac{E\dot{e}}{1+\nu}\frac{\partial P(s,t)}{\partial s}+e^{-\beta\Delta E(s)}P(s,t)=\dot{N}\delta(s).$$

Substituting $s=(\frac{2}{3})^{1/2}\sigma$ in this formula and defining $P(\sigma,t)=(\frac{2}{3})^{1/2}P(s,t)$, so that

$$\int_{-\sigma_a}^{\sigma_a} d\sigma\ P(\sigma,t)=\int_{-s_0}^{s_0} ds\ P(s,t)=1,$$

gives Eq. (20).

As a second application, consider a spherical cavity in a solid, and assume that a time-dependent pressure acts on the cavity walls. This will give rise to a displacement field in the solid of the form

$$u_i(\mathbf{x},t)=x_i u(r,t)/r, \tag{57}$$

where $r=0$ is at the origin of the cavity. The strain deviator

$$e_{ij}=\tfrac{1}{2}(u_{ij}+u_{j,i})-\tfrac{1}{3}u_{k,k}\delta_{ij}=eM_{ij}, \tag{58}$$

where

$$e=(\tfrac{2}{3})^{1/2}r\frac{\partial}{\partial r}\left(\frac{u}{r}\right), \tag{59}$$

and

$$M_{ij}=(\tfrac{1}{6})^{1/2}\left(3\frac{x_ix_j}{r^2}-\delta_{ij}\right),\quad M_{ij}M_{ij}=1. \tag{60}$$

Thus $\dot{e}_{ij}$ is again of the form Eq. (49) and we therefore know at once that $P(s_{ij},t)$ can be written in the form Eq. (51) where $P(s,t)$ satisfies Eq. (56). To obtain the displacement field we must solve the equation of motion

$$\rho\frac{\partial^2 u_i}{\partial t^2}=\langle\sigma_{ij}\rangle_{,j}, \tag{61}$$

where

$$\langle\sigma_{ij}\rangle=\langle s_{ij}\rangle+\tfrac{1}{3}\sigma_{kk}\delta_{ij}.$$

Note that in the earlier application (uniaxial tension) $\dot{\varepsilon}$ and $\langle\sigma\rangle$ were independent of $\mathbf{x}$, and it was not necessary to consider Eq. (61). Noting that $\sigma_{kk}=E\varepsilon_{kk}/(1-2\nu)$, and

$$\varepsilon_{kk,i}=u_{k,ki}=\frac{x_i}{r}\frac{\partial}{\partial r}\left[\frac{3u}{r}+r\frac{\partial}{\partial r}\left(\frac{u}{r}\right)\right],$$

and

$$\langle\sigma_{ij}\rangle_{,j}=(M_{ij}\langle s(r,t)\rangle)_{,j}=(\tfrac{2}{3})^{1/2}\frac{x_i}{r}\left(3\frac{\langle s\rangle}{r}+\frac{\partial}{\partial r}\langle s\rangle\right)$$

Eq. (61) gives

$$\rho\frac{\partial^2 u}{\partial t^2}=\left(\frac{2}{3}\right)^{1/2}\left(3\frac{\langle s\rangle}{r}+\frac{\partial}{\partial r}\langle s\rangle\right)+\frac{E}{3(1-2\nu)}\frac{\partial}{\partial r}\left[\frac{3u}{r}+r\frac{\partial}{\partial r}\left(\frac{u}{r}\right)\right]. \quad (62)$$

To solve this equation we need the nonlinear functional relation between $\langle s\rangle$ and $\dot{e}$, which follows from Eq. (56). As a simple illustration, let us consider the linear response case (linear viscoelasticity) where

$$\langle\tilde{s}\rangle=\frac{(-i\omega)\tilde{e}E}{(1+\nu)[-i\omega+\nu_0\exp(-\beta\epsilon)]} \quad (63)$$

with $\tilde{e}$ the time-Fourier transform of $e(r,t)$. If we write $u=\partial\phi/\partial r$ and if we substitute Eq. (63) in Eq. (62) and use Eq. (59) we get, after some simplifications,

$$\rho\omega^2\tilde{\phi}+\frac{E}{3}\left(\frac{1}{1-2\nu}+\frac{-2i\omega/(1+\nu)}{-i\omega+\nu_0\exp(-\beta\epsilon)}\right)\times\left(\frac{3}{r}+r\frac{d}{dr}\frac{1}{r}\right)\frac{d}{dr}\tilde{\phi}=0. \quad (64)$$

This equation has the solution

$$\tilde{\phi}=e^{ikr}\tilde{\phi}_0/r. \quad (65)$$

Substituting Eq. (65) in Eq. (64) gives, after some simplification,

$$k^2=\left(\frac{\omega}{c_L}\right)^2\frac{1-3/[2i\omega\tau(1+\nu)]}{1-1/[2i\omega\tau(1-\nu)]},$$

where

$$c_L=\left(\frac{E(1-\nu)}{\rho(1+\nu)(1-2\nu)}\right)^{1/2}$$

is the longitudinal sound velocity, and the relaxation time $\tau=\eta/E$, where η is defined by Eq. (39). When $\tau\to\infty$ then $k\to\omega/c_L$ and in this limiting case the solution Eq. (65) describes undamped, spherical (longitudinal) elastic waves emitted from the cavity. When η is finite (but small) the same picture is valid, except that now the emitted sound waves are damped. In the more general case where the displacement u is so large that the linear response assumption is invalid, the deformation field will in general consist of an inner spherical shell around the cavity where the solid has undergone plastic deformation, surrounded by another spherical shell where nonlinear viscoelasticity (or viscoplasticity) prevails and an outer region (extending to infinity) where the linear viscoelastic approximation is accurate, see Fig. 11(a). This complex deformation field is in principle contained in the equations presented above, although the calculations would be rather involved. Nevertheless, a general understanding of the nature of the solutions to problems like this is of great importance in many important applications, e.g., concerning the magnitude of the fracture energy and the deformation field in the vicinity of a crack tip, see Fig. 11(b).

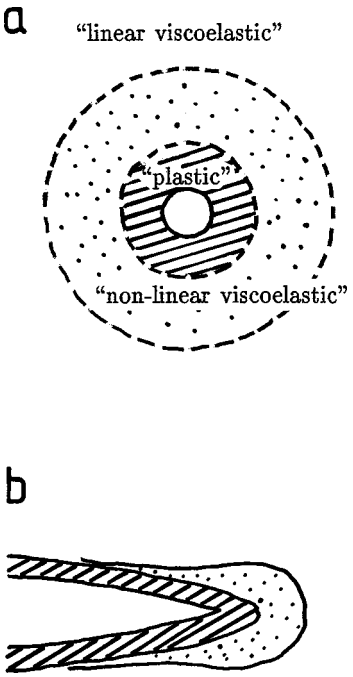

FIG. 11. (a) A spherical cavity in a solid with a time varying pressure gives rise to plastic and viscoelastic (or viscoplastic) deformation of the solid. (b) The deformation field around a propagating crack.

X. COMMENTS

In the theory developed in Secs. II and III, we have made a few assumptions and approximations, which we now comment on. We have treated the media as isotropic, which usually is a good approximation for glassy atomic solids even at the short length scales (say $\sim$ 100 Å) relevant for the present applications. As a result, application of von Mises type of yield criteria to the stress blocks should be accurate. In fact, molecular dynamics calculations have shown that the von Mises yield criteria may hold at least approximately even for single crystals when they are exposed to rapidly (in space) varying stress fields. Thus computer calculations by Landman *et al.*[11] have shown that the yielding of nanoscale junctions between a Ni-tip and a gold substrate (single crystals) occurs when the quantity $(3s_{ij}s_{ij}/2)^{1/2}$ reaches a critical value $\sigma_a\approx 5\times 10^9$ N/m^2 (which, for reasons discussed in Ref. 2, is much higher than the macroscopic yield stress of gold).

Another assumption made above is that when a stress block yields, the local shear stress drops to zero. This is unlikely to be true in general. Thus during the nanoscale yielding processes discussed above the quantity $(3s_{ij}s_{ij}/2)^{1/2}$ changed (abruptly) from 5 GPa to 3 GPa in the region where the yield occurred. However, it is easy to modify the theory to take into account only a partial release of shear stress during local yield.

We have assumed a well-defined activation energy ϵ. In reality one may expect a distribution of activation barriers, and a corresponding distribution of local yield stresses. We also note that the activation energy ϵ for plastic flow has a weak dependence on the hydrostatic pressure, i.e., the standard statement that the plastic yield condition only depends on the stress deviator is not completely rigorous.

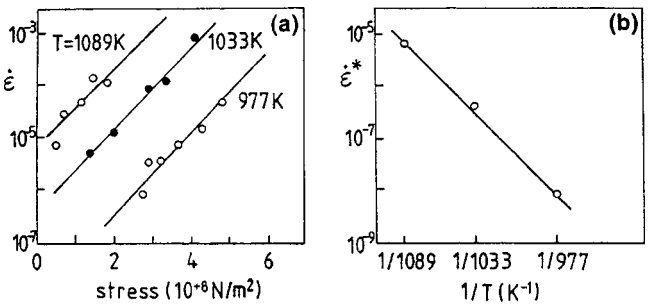

FIG. 12. (a) Steady state creep rate $\dot{\varepsilon}$ (in units of h^{-1}) for the superalloy Waspaloy as a function of stress. (b) Strain-rate $\dot{\varepsilon}^*$ (in units of h^{-1}) as a function of the inverse of the temperature, $1/T$ ($\dot{\varepsilon}^*$ is the strain rate extrapolated to zero stress). From Ref. 12.

XI. APPLICATIONS

A. Thermally activated creep in metals

The pinning energy for dislocations in metals are typically of order $\epsilon \sim 1$ eV. In order to reduce the creep rate as much as possible, the pinning energy ϵ should be as large as possible. Special ''superalloys'' have been developed, which exhibit small creep even at relative high temperatures, and which are used, e.g., for jet engine turbine blades. Figure 12(a) shows the relation between the strain rate $\dot{\varepsilon}$ and the stress σ for three different temperatures for a nickel-based superalloy (Waspaloy).[12] Note that σ depends linearly on $\ln \dot{\varepsilon}$ in accordance with Eq. (37). In order to determine the activation energy ϵ we write Eq. (37) in the form

$$\sigma = \sigma_c \left(1 + \frac{k_B T}{\epsilon} \ln(\dot{\varepsilon}/\dot{\varepsilon}_0) \right), \tag{66}$$

where $\sigma_c = \sigma_a/2$ is the macroscopic yield stress and

$$\dot{\varepsilon}_0 = \frac{8 \nu_0 (1+\nu) \sigma_c}{3 E \beta \epsilon}. \tag{67}$$

Thus, if the curves in Fig. 12(a) are extrapolated to $\sigma = 0$, the resulting creep rate $\dot{\varepsilon} = \dot{\varepsilon}^*$ should satisfy

$$1 + \frac{k_B T}{\epsilon} \ln(\dot{\varepsilon}^*/\dot{\varepsilon}_0) = 0,$$

or

$$\ln(\dot{\varepsilon}^*/\dot{\varepsilon}_1) = \ln(\dot{\varepsilon}_0/\dot{\varepsilon}_1) - \epsilon/k_B T, \tag{68}$$

where $\dot{\varepsilon}_1$ is an arbitrarily chosen (e.g., $\dot{\varepsilon}_1 = 1\ s^{-1}$) reference strain rate. In a typical case $\dot{\varepsilon}_0 \sim 10^8\ s^{-1}$ so that, if $\dot{\varepsilon}_1 \sim 1\ s^{-1}$, even if $\dot{\varepsilon}_0$ is proportional to T, the temperature dependence of $\ln(\dot{\varepsilon}_0/\dot{\varepsilon}_1)$ is completely negligible. Thus, from Eq. (68) we expect a linear relation between the $\ln(\varepsilon^*/\varepsilon_1)$ and $1/T$ as is indeed observed, see Fig. 12(b). From the slope of the curve in Fig. 12(b) we deduce $\epsilon \approx 5.5$ eV, which is higher than for ''normal'' steel. Using Eq. (8(b)) one can calculate the diameter D of a stress block, which turns out to be about $D \sim 30$ Å. This gives $v_0 \sim c/2\pi D \sim 10^{11}\ s^{-1}$ and $\dot{\varepsilon}_0 \sim 10^8\ s^{-1}$.

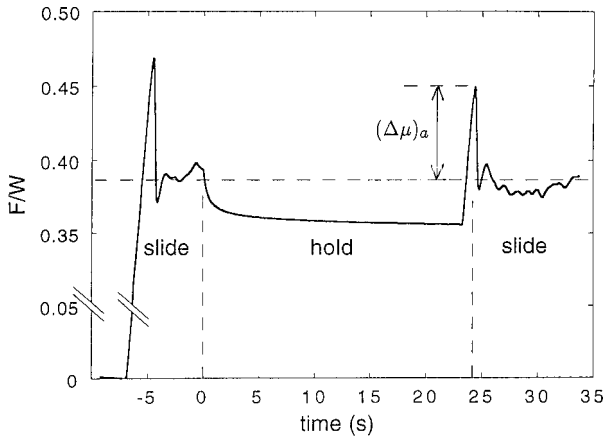

FIG. 13. Experimental trace of the static force measurement according to the stressed aging procedure described in the text. Note the break in the vertical scale. From Ref. 15.

B. Creep enhancement of the area of real contact

When a solid block is placed on a substrate, plastic deformation usually occurs in the contact areas, and a short time after contact the local stresses equals the plastic yield stress. Immediately after the rapid plastic deformations the stress blocks in the vicinity of the contact area will be in a ''critical'' state with a distribution of local stresses such that some stress blocks are almost ready to undergo plastic deformation. This implies that thermal processes will be of crucial importance; slow relaxation (creep) will occur and the contact area will increase slowly with time.

The theory developed above can be used to study how the area of real contact depends on time t and one can show that $A = A_0[1 + B \ln(1 + t/\tau_0)]$ to leading order in $B = k_B T/\epsilon$ (Refs. 2 and 13). This logarithmic increase in the contact area with the time of stationary contact has been observed for many systems (see Ref. 14) and is of crucial importance for dry friction dynamics.

C. Sliding friction

Recently Berthoud *et al.*[15] have performed friction experiments with poly(methyl metacrylate) (PMMA) and polystyrene (PS). They observed that the static friction force depends on the time of stationary contact. Well-defined measurements were performed using *free aging* and *stressed aging*. In both cases the top block was first sliding with a constant velocity v. In *free aging* the driving stage was suddenly reversed in order to quickly unload the slider, so that the waiting stage essentially corresponded to zero tangential force. After a fixed time period τ the loading is resumed with the same velocity v as before stop and the static friction is determined at the maximum of the ''striction'' spike. In *stressed aging* the driving stage is suddenly stopped and kept fixed. After a fixed time delay τ the loading is assumed with the same velocity as before the stop, see Fig. 13. The height of the ''striction'' spikes above that of the steady state sliding is denoted by $(\Delta\mu_a)$ and $(\Delta\mu)_b$ for stressed and free aging, respectively. It was observed that the ratio $(\Delta\mu)_a/(\Delta\mu)_b$ is *temperature independent* and equal to 2.1 and 1.3 for PS and PMMA, respectively. Thus the static friction force increases faster with the time of stationary contact during stressed aging.

As pointed out by Berthoud *et al.*, there are two (obvious) possible explanations for the observed effect. First, the area of real contact may increase faster for a stressed block than for an unstressed block. This follows from the fact that time-dependent plastic deformation (creep) may occur faster in a junction that is exposed to a tangential shear stress in addition to the normal stress from the load of the block. However, after a detailed study Berthoud *et al.*, concluded that this effect is unlikely to account for the difference between the two aging processes (see Ref. 15). A second mechanism suggested in Ref. 15 is related to the study presented in Sec. VIII. During steady sliding at low sliding velocity a wide distribution of tangential stresses will occur at the sliding interface. Surface asperities[16] or stress domains[5] in the contact areas form a wide distribution of elastically deformed states which during ''stop'' will slowly relax towards the equilibrium (unstressed) state. From the study in Sec. VIII we expect the relaxation to be more effective for stressed aging than for free aging, i.e., $(\Delta\mu)_a > (\Delta\mu)_b$ as indeed observed experimentally for the systems studied by Berthoud *et al.* However, from the results presented in Sec. VIII one would expect the ratio $(\Delta\mu)_a/(\Delta\mu)_b$ to depend on the temperature in contrast to the experimental data of Berthoud *et al.* I have performed computer simulations for other combinations of the spring constants k_1 and k_2 (see Sec. VIII and Fig. 4), in particular for $k_2=0$, which may be taken to correspond to noninteraction surface asperities, but I always observe a strong temperature dependence of $(\Delta\mu)_a/(\Delta\mu)_b$, similar to the result presented in Fig. 10. Such a temperature dependence is also expected from simple physical arguments. Thus, the discrepancy between theory and experiment is very puzzling, and it is clear that the exact origin of the increase of the static friction force during stationary contact is not well understood at present.

D. Thermally activated creep of clayey samples

The theory developed above seems to be valid also for granular multicomponent systems like natural soils.[17] Creep and relaxation has been studied for natural or reconstituted samples of water-saturated clay or similar densified mud. These systems consist of grains the size of which ranges from about 10^{-7} m to 10^{-5} m; the mineral is mainly silicate. Experiments are performed on samples confined within cylindrical or plane walls.

1. Stationary creep

Stationary creep experiments are performed with constant volume and skeleton pressure components. The cylindrical sample is shortened at a constant rate $\dot{\varepsilon}=\dot{l}/l$, while the system expands in the other two spatial directions so that the volume is constant. After a transition time period the system reaches a stationary state where the stress does not depend on the initial state of the system, and where the difference between the skeleton pressures p_1 and p_2, along the cylinder axis and the radial direction, respectively, satisfies

$$p_1-p_2=C\left(1+\frac{k_BT}{\epsilon}\ln(\dot{\varepsilon}/\dot{\varepsilon}_0)\right),$$

where C and ϵ are temperature independent, while the reference strain rate $\dot{\varepsilon}_0$ is proportional to T.

2. Volumetric creep

Volumetric creep is observed by keeping the external pressure constant. The void ratio $e=(1-\alpha)/\alpha$, where α is the solid volume fraction, is found to have the time dependence

$$e(0)-e(t)=C'\frac{k_BT}{\epsilon}\ln(1+t/\tau),$$

where C' and ϵ are independent of the temperature T.

3. Relaxation

Relaxation is observed by keeping cuboidal samples fixed within plates after different deformation histories. The skeleton pressure components p_i return to equilibrium according to characteristic relaxation curves when plotting p_i as a function of $\ln(t/\tau)$, where the relaxation time τ is defined by extrapolating the straight section of this plot to the equilibrium value. It is found that τ is independent of the deformation history.

These experimental results can be understood based on the theoretical results presented above and in Ref. 5. Thus, the particle system deforms slowly (creep and relaxation) by (a) thermally activated slip between particles in response to the tangential surface stresses in the contact areas, as described by the theory presented in Ref. 5, and by (b) time-dependent plastic deformation of the solid particles (mainly due to the perpendicular contact stresses), as described by the theory above. Both processes gives relaxation $\sim\ln(1+t/\tau)$ and creep rates $\sim\ln(\dot{\varepsilon}/\dot{\varepsilon}_0)$, with the same temperature dependence as observed experimentally.

The stationary creep results presented above are not valid if the driving stress and resulting strain rate is extremely low. In the latter case the theory predicts that the strain rate should be directly proportional to the stress. This limiting case cannot be probed in laboratory experiments because of the low strain rates involved, but may show up in nature on geological time scales as clay deposits can exist for millions of years.

E. Other manifestations of creep

We give here a few other manifestations of time-dependent plastic deformation. First, consider a block of glass with a gas bubble. Glass is usually considered as a brittle material but the response to a small stress is not brittle fracture but slow creep motion. Thus the air bubble moves slowly upwards and on the time scale of 1000 year glass behaves as a typical viscous fluid. Similarly, old glass windows are thicker at the lower edges than at the upper edges because of a slow flow of the glass due to the gravitational force. In both these applications the driving forces (or stresses) are so small that the stress σ is likely to be linearly related to the strain rate $\dot{\varepsilon}$, as expected for a fluid. As another application, consider the earth's crust which is continuously exposed to fluctuating stresses. This gives rise to a slow creep motion but in most cases the stress and strain rates are so high that the relation $\dot{\varepsilon}=f(\sigma)$ is nonlinear. Thus one has

discovered mine channels in Yugoslavia from Roman times, where the channel height has been reduced by creep to the extent that it is impossible for humans to move in them. Another proof that stone creeps under load is the now strongly plastically deformed Abraham spring close to Jerusalem. Other manifestations of creep are the formation of mountains (over millions of years) and the creep motion at fault lines.

XII. SUMMARY AND CONCLUSION

I have developed a general model of time-dependent plastic deformation of solids. The theory is centered around the concept of a stress probability distribution function P. Plastic deformation is considered to involve local shear yielding of small volume elements (stress blocks). A stress block yields either as a result of being pulled over the barrier to shear yielding by an external applied stress, or it jumps over the barrier due to a thermal fluctuation. In a general case both these mechanisms operate simultaneously; this is the mechanism of stress-aided thermal flow considered in a classic paper by Eyring. Analytical results have been worked out in some limiting cases and are in good agreement with experimental data.

ACKNOWLEDGMENTS

I would like to thank G. Eilenberger for useful discussions related to Appendix C. I thank G. Gudehus for discussions about plastic deformation and creep in granular materials (e.g., clayey samples). I thank T. Baumberger for sending me a preprint of Ref. 12 and for allowing me to use a figure from his experiments on sliding friction. I also thank J. S. Langer for supplying a copy of Ref. 4 prior to publication and for drawing my attention to the work of Argon *et al.*, Ref. 3. This work was sponsored by an BMBF grant related to the German-Israeli Project Cooperation ''Novel Tribological Strategies from the Nano- to Meso-Scales.''

APPENDIX A

We consider a cuboidal solid block and assume that the surfaces of the block are clamped and displaced so that the stress in the block equals σ_{ij} everywhere. In this appendix we will estimate the activation barrier ΔE for local shear ''melting.'' Let us consider a stress domain, in the solid block. The stress in the stress domain is assumed to be constant and given by $\sigma_{ij}=s_{ij}+p\,\delta_{ij}$. We estimate the elastic barrier ΔE necessary to increasing the local stress from σ_{ij} to the value $\sigma^0_{ij}=s^0_{ij}+p^0\delta_{ij}$. In the applications presented in this paper we have $p=p^0$ since the local shear ''melting'' does not depend on the hydrostatic pressure (the yield criteria depends only on the stress deviator s_{ij}). Physically, the increase in the local stress at a stress domain can be considered as the result of a thermal fluctuation. This can be described by a fluctuating force field $\mathbf{f}(\mathbf{x},t)$. In the present case we will assume that $\mathbf{f}(\mathbf{x},t)$ corresponds to a stress acting on the surface of the stress block [i.e., $\mathbf{f}\sim\delta(r-R)$]. The minimum work necessary for this fluctuating force to increase the stress in the stress domain from σ_{ij} to σ^0_{ij} can be estimated using $\Delta E=E_2-E_1$, where E_2 is the total elastic energy in the body under the assumption that the stress in the stress block equals σ^0_{ij}, while far away from the stress block the stress equals σ_{ij}. E_1 is the elastic energy stored in the body when the stress equals σ_{ij} everywhere. When calculating E_2 we assume that the stress satisfies the equation

$$\sigma_{ij,j}=0 \tag{A1}$$

everywhere, except at the surface of the block, where σ_{ij} is discontinuous, while the displacement field u_i is continuous. We get

$$E_2=\tfrac{1}{2}\int_V d^3x\,\sigma_{ij}\varepsilon_{ij}\,. \tag{A2}$$

Substituting

$$\varepsilon_{ij}=\tfrac{1}{2}\,(u_{i,j}+u_{j,i})$$

in Eq. (A2), performing a partial integration, and using Eq. (A1) gives

$$E_2=\tfrac{1}{2}\int_{S_1} d^2x\,\sigma_{ij}u_i n_j+\tfrac{1}{2}\int_S d^2x(\sigma^-_{ij}-\sigma^+_{ij})u_i n_j\,, \tag{A3}$$

where S_1 is the outer (clamped) surface of the body and S the surface of the stress domain. In Eq. (A3) n_i denote the unit vector normal to the surface S (and S_1) pointing away from the interior, and σ^-_{ij} and σ^+_{ij} denote the stress tensor just inside and outside the surface S, respectively. Since the outer surface of the body is clamped, the displacement u_i at the surface S_1 does not change during the transition, and since (to be proved below) the correction to the stress field from the stress domains decay as $1/r^3$ with the distance from the stress domain, it follows that in the limit of a very large body the first integral in Eq. (A3) is unchanged during the transition. Thus the change in the elastic energy is

$$\Delta E=\tfrac{1}{2}\int_S d^2x(\sigma^-_{ij}-\sigma^+_{ij})u_i n_j\,. \tag{A4}$$

Let us assume that a stress domain is a spherical volume element with radius R, and introduce a coordinate system with the origin at the center of the sphere. The ''initial'' displacement field u_i in the solid is given everywhere by

$$u_i=\frac{1}{E}[(1+\nu)s_{ij}x_j+(1-2\nu)px_i],$$

which corresponds to the initial stress tensor

$$\sigma_{ij}=s_{ij}+p\,\delta_{ij}\,,$$

where s_{ij} and p are constants. The ''final'' displacement field u^0_i for $r<R$ is given by

$$u^0_i=\frac{1}{e}[(1+\nu)s^0_{ij}x_j+(1-2\nu)p^0x_i],$$

which corresponds to the final stress tensor

$$\sigma^0_{ij}=s^0_{ij}+p^0\delta_{ij}\,,$$

where s^0_{ij} and p^0 are constants. For $r>R$ we have

$$u_i^0=\frac{1}{E}[(1+\nu)s_{ij}x_j+(1-2\nu)px_i]+u_i^{(1)}+u_i^{(2)},$$

where $u_i^{(1)}$ and $u_i^{(2)}\to 0$ as $r\to\infty$ and satisfies $\nabla\times\mathbf{u}^{(1)}=\mathbf{0}$ and $\nabla^2\nabla\cdot\mathbf{u}^{(2)}=0$. The relevant solutions to these equations can be written as

$$u_i^{(1)}=ax_i/r^3$$

and

$$u_i^{(2)}=Aa_{ij}\nabla_j\frac{1}{r}+Ba_{jk}\nabla_i\nabla_j\nabla_k\frac{1}{r}+Ca_{jk}\nabla_i\nabla_j\nabla_k r.$$

These displacement fields satisfy Eq. (A1) if

$$A=-4C(1-\nu).$$

The condition that u_i^0 must be continuous for $r=R$ gives

$$a=(R^3/E)(1-2\nu)(p^0-p),$$

$$A=-\frac{20(1-\nu^2)R^3}{(16-20\nu)E},$$

$$B=\frac{(1+\nu)R^5}{(16-20\nu)E},$$

$$a_{ij}=s_{ij}^0-s_{ij}.$$

It is now straight forward to calculate the strain

$$\varepsilon_{ij}=\tfrac{1}{2}(u_{i,j}^0+u_{j,i}^0)$$

and from it the stress tensors σ_{ij}^+ and σ_{ij}^- just outside and inside the boundary $r=R$ of the stress domain. Substituting the result in Eq. (A4), assuming $p=p^0$, gives after some simplifications

$$\Delta E=\frac{5\pi R^3(1-\nu^2)}{E(4-5\nu)}(s_{ij}^0-s_{ij})s_{ij}^0.$$

APPENDIX B

We consider stationary creep. In this case the stress probability distribution function is given by Eq. (33):

$$P(\sigma)=C\theta(\sigma)\exp\Bigg(-[2\nu_0(1+\nu)/3E\dot\varepsilon]\int_0^\sigma d\sigma'\times\exp[-\beta\epsilon(1-\sigma'/\sigma_a)]\Bigg)$$
$$=C\theta(\sigma)e^{-\alpha\exp(-\beta\epsilon)[\exp(\beta\epsilon\sigma/\sigma_a)-1]},\qquad\text{(B1)}$$

where the number C is determined by the normalization condition (2) and where $\alpha=2\nu_0(1+\nu)\sigma_a/(3E\dot\varepsilon\beta\epsilon)$. The average stress is determined by the equation

$$\langle\sigma\rangle=\frac{\int_{-\sigma_a}^{\sigma_a}d\sigma\,\sigma P(\sigma)}{\int_{-\sigma_a}^{\sigma_a}d\sigma\,P(\sigma)}.\qquad\text{(B2)}$$

Let us first consider the large-$\dot\varepsilon$ limit. Assume that $\alpha\ll 1$ and $\beta\epsilon\gg 1$. In this case, to leading order in α, Eq. (B1) gives

$$P(\sigma)\sim C\theta(\sigma)[1-\alpha e^{-\beta\epsilon}(e^{\beta\epsilon\sigma/\sigma_a}-1)].$$

Substituting this in Eq. (B2) gives to leading order in α

$$\langle\sigma\rangle=\frac{\sigma_a}{2}\left[1+\alpha\int_0^{\sigma_a}\frac{d\sigma}{\sigma_a}\left(1-\frac{2\sigma}{\sigma_a}\right)e^{-\beta\epsilon}(e^{\beta\epsilon\sigma/\sigma_a}-1)\right].$$

Performing the integral gives for $\alpha\ll 1$ and $\beta\epsilon\gg 1$:

$$\langle\sigma\rangle\sim\frac{\sigma_a}{2}\left(1-\frac{\alpha}{\beta\epsilon}\right)=\frac{\sigma_a}{2}\left[1-\frac{2\nu_0(1+\nu)\sigma_a}{3E\dot\varepsilon(\beta\epsilon)^2}\right].\qquad\text{(B3)}$$

Next, let us consider small shear rates. Assume that $\alpha\gg 1$ but $\alpha\exp(-\beta\epsilon)\ll 1$. Let us consider the integral I, which occur in the nominator of Eq. (B2):

$$I=\int_0^{\sigma_a}d\sigma\,\sigma e^{-\alpha\exp(-\beta\epsilon)[\exp(\beta\epsilon\sigma/\sigma_a)-1]}=\sigma_a^2(1/2+J),$$

where

$$J=\int_0^{\sigma_a}d(\sigma/\sigma_a)(\sigma/\sigma_a)(e^{-\alpha\exp(-\beta\epsilon)[\exp(\beta\epsilon\sigma/\sigma_a)-1]}-1).$$

Now, it is easy to see that the main contribution to J comes from when $\sigma\approx\sigma_a$ Hence, if we write $\sigma=\sigma_a(1-\xi)$, the dominant contribution comes from $\xi\approx 0$. Thus

$$J=\int_0^1 d\xi(1-\xi)(e^{-\alpha[\exp(-\beta\epsilon\xi)-\exp(-\beta\epsilon)]}-1)$$
$$\approx\int_0^1 d\xi(e^{-\alpha\exp(-\beta\epsilon\xi)}-1).$$

Let us put $\eta=\exp(-\beta\epsilon\xi)$ so that

$$J=\int_{e^{-\beta\epsilon}}^1\frac{d\eta}{\beta\epsilon\eta}(e^{-\alpha\eta}-1).$$

Since we have assumed $\alpha\gg 1$ and $\exp(-\beta\epsilon)\ll 1$ the leading contribution to J becomes

$$J\sim-\int_{1/\alpha}^1\frac{d\eta}{\beta\epsilon\eta}=-\frac{1}{\beta\epsilon}\ln\alpha.$$

The denominator in Eq. (B2) can be evaluated in a similar manner as the nominator and equals $\sigma_a(1+J)$. Hence, to leading order the sliding friction is given by

$$\langle\sigma\rangle=\frac{1}{2}\sigma_a\frac{1+2J}{1+J}\sim\frac{\sigma_a}{2}(1+J)$$
$$=\frac{\sigma_a}{2}\left[1+\frac{1}{\beta e}\ln\left(\frac{3E\dot\varepsilon\beta\epsilon}{2\nu_0(1+\nu)\sigma_a}\right)\right].\qquad\text{(B4)}$$

In the extreme low-$\dot\varepsilon$ limit, where $\alpha\exp(-\beta\epsilon)\gg 1$, only the $\sigma\approx 0$ region in the integral in the exponent of Eq. (B1) will contribute, and we can approximate

$$P(\sigma)\sim C\theta(\sigma)e^{-\alpha\beta\epsilon(\sigma/\sigma_a)\exp(-\beta\epsilon)}.$$

Substituting this in Eq. (B2) gives

$$\langle\sigma\rangle\sim(\sigma_a/\alpha\beta\epsilon)e^{\beta\epsilon}=\frac{3E\dot{\varepsilon}}{2\nu_0(1+\nu)}e^{\beta\epsilon}. \tag{B5}$$

Note that $\langle\sigma\rangle\ll\sigma_a$ and that the stress is proportional to the strain rate.

APPENDIX C

In this appendix I study the probability distribution function $P(\sigma,t)$ for a solid block exposed to an oscillatory strain of arbitrary amplitude. The equation of motion is given by Eq. (20) with $e=e_0\sin(\omega t)$ and $\dot{e}=\omega e_0\cos(\omega t)$:

$$\frac{\partial P}{\partial t}+a\cos(\omega t)\frac{\partial P}{\partial\sigma}+\nu_0 e^{-\beta\Delta E(\sigma)}P-\dot{N}\delta(\sigma)=0, \tag{C1}$$

where we have defined

$$a=\frac{3E\omega e_0}{2(1+\nu)}.$$

The general solution to Eq. (C1) has the form

$$\begin{aligned}P=&f[\sigma-\sigma_1\sin(\omega t)]\\&\times\exp\left(-\nu_0\int_0^t dt'\exp[-\beta\epsilon(1-|\sigma-\sigma_1\sin(\omega t)\right.\\&\left.+\sigma_1\sin(\omega t')|/\sigma_a)]\right)+\frac{1}{\sigma_a}\left[\exp\left(\int_0^t dt'G(t')\right.\right.\\&\left.\left.\times\delta[\sigma-\sigma_1\sin(\omega t)+\sigma_1\sin(\omega t')]\right)-1\right]\\&\times\exp\left(-\nu_0\int_0^t dt'\exp[-\beta\epsilon(1-|\sigma-\sigma_1\sin(\omega t)\right.\\&\left.+\sigma_1\sin(\omega t')|/\sigma_a)]\right),\end{aligned} \tag{C2}$$

where $\sigma_1=a/\omega$ and where $G(t)$ must be chosen so that the normalization condition (C7) is satisfied for all times. Note that $f(\sigma)$ is the initial (arbitrary) stress distribution. Now, it is clear from the underlying physical problem that for large times the function P must converge towards a unique ''fixed-point'' solution, which is independent of the initial probability distribution $f(\sigma)$, and which must be periodic in time with the period $T=2\pi/\omega$. In fact, it follows directly from Eq. (C2) that for large times

$$\begin{aligned}P=&\frac{1}{\sigma_a}\exp\left(\int_0^t dt'G(t')\delta[\sigma-\sigma_1\sin(\omega t)+\sigma_1\sin(\omega t')]\right)\\&\times\exp\left(-\nu_0\int_0^t dt'\exp[-\beta\epsilon(1-|\sigma-\sigma_1\sin(\omega t)\right.\\&\left.+\sigma_1\sin(\omega t')|/\sigma_a)]\right),\end{aligned}$$

which must satisfy $P(\sigma,t)=P(\sigma,t+T)$. This last condition is possible only if

$$\begin{aligned}&\nu_0\int_0^T dt'\exp[-\beta\epsilon(1-|\sigma-\sigma_1\sin(\omega t)\\&\quad+\sigma_1\sin[\omega(t+t')]|/\sigma_a)]\\&=\int_0^T dt'G(t+t')\delta\{\sigma-\sigma_1\sin(\omega t)+\sigma_1\sin[\omega(t+t')]\}.\end{aligned} \tag{C3}$$

Now, note that the left-hand side of this equality is always nonzero, while the right-hand side vanishes if $|\sigma-\sigma_1\sin(\omega t)|>\sigma_1$. This implies that if this inequality is satisfied we must have $P=0$ in order not to have a contradiction. In fact, it is easy to understand physically why $P=0$ if $|\sigma-\sigma_1\sin(\omega t)|>\sigma_1$. Next, let us consider $|\sigma-\sigma_1\sin(\omega t)|<\sigma_1$. Now, in the interval $0<t'<T$ the equation

$$\sigma-\sigma_1\sin(\omega t)+\sigma_1\sin[\omega(t+t')]=0 \tag{C4}$$

has, as a function of t', two solutions, which we denote by $\tau_1(\sigma,t)$ and $\tau_2(\sigma,t)$. Note that

$$\cos\omega(t+\tau_1)=-\cos\omega(t+\tau_2).$$

Using this equation we get

$$\begin{aligned}I=&\int_0^T dt'G(t+t')\delta\{\sigma-\sigma_1\sin(\omega t)+\sigma_1\sin[\omega(t+t')]\}\\=&\frac{1}{\sigma_1\omega|\cos\omega(t+\tau_1)|}[G(t+\tau_1)+G(t+\tau_2)].\end{aligned}$$

Now, up to this point σ and t are arbitrary. Let us now choose $\sigma=0$ in which case the solutions to Eq. (C3) and Eq. (C4) are $\tau_1=0$ and $\tau_2=T/2-2t$, where we have assumed $t<T/4$. This gives

$$I=\frac{1}{\sigma_1\omega|\cos\omega t|}[G(t)+G(T/2-t)].$$

Substituting this in Eq. (C3) and using that $G(T/2-t)=G(-t)$ gives

$$\begin{aligned}&\nu_0\int_0^T dt'\exp(-\beta\epsilon\{1-|\sigma_1\sin(\omega t)\\&\quad-\sigma_1\sin[\omega(t+t')]|/\sigma_a\})\\&=\frac{1}{\sigma_1\omega|\cos\omega t|}[G(t)+G(-t)].\end{aligned} \tag{C5}$$

Let us write $G(t)=G_e(t)+G_o(t)$, where $G_e(t)=G_e(-t)$ is an even function of t and $G_0(t)=-G_o(-t)$ is an odd function of t. Using Eq. (C5) gives

$$\begin{aligned}G_e(t)=&\frac{\sigma_1\omega\nu_0}{2}|\cos(\omega t)|\\&\times\int_0^T dt'\exp\{-\beta\epsilon[1-(\sigma_1/\sigma_a)|\sin(\omega t)\\&-\sin\omega(t+t')]\}.\end{aligned} \tag{C6}$$

The function $G_o(t)$ is determined by the normalization condition

$$\int_{-\sigma_a}^{\sigma_a} d\sigma\, P(\sigma,t) = 1, \tag{C7}$$

which must be satisfied for all times t. When this equation is satisfied, the relation between the stain $\varepsilon(t)$ and the stress is obtained from

$$\langle \sigma \rangle = \int_{-\sigma_a}^{\sigma_a} d\sigma\, \sigma P(\sigma,t). \tag{C8}$$

The derivation of the relation between stress and strain using the equations above is in progress, and will be reported on elsewhere.

[1] J. H. Hollomon and C. Zener, J. Appl. Phys. **17**, 69 (1946).
[2] See, e.g., B. N. J. Persson, *Sliding Friction: Physical Principles and Applications* (Springer, Heidelberg, 1998).
[3] A. S. Argon, V. V. Bulatov, P. H. Mott, and U. W. Suter, J. Rheol. **39**, 377 (1995).
[4] M. L. Falk and J. S. Langer, Phys. Rev. E **57**, 7192 (1998).
[5] B. N. J. Persson, Phys. Rev. B **51**, 13 568 (1995).
[6] See, e.g., B. N. J. Persson, Surf. Sci. Rep. **15**, 1 (1992).
[7] T. Egami and V. Vitek, in *Amorphous Materials: Modeling of Structure and Properties*, edited by V. Vitek (AIME, Warrendale, PA, 1983).
[8] D. N. Theodorou and U. W. Suter, Macromolecules **18**, 1467 (1985); **19**, 139 (1986); **19**, 379 (1986).
[9] S. G. Corcoran, R. J. Colton, E. T. Lilleodden and W. W. Gerberich, Phys. Rev. B **55**, R16 057 (1997).
[10] See, e.g., F. A. McClintock and A. S. Argon, *Mechanical Behavior of Materials* (Addison-Wesley, Reading, MA, 1966).
[11] U. Landman, W. D. Luedtke, N. A. Burnham, and R. J. Colton, Science **248**, 454 (1990).
[12] D. P. Moon, R. C. Simon, and R. J. Favor, *The Elevated-Temperature Properties of Selected Superalloys* (ASTM, Philadelphia, 1968), p. 335.
[13] T. Baumberger, Solid State Commun. **102**, 175 (1997).
[14] J. H. Dieterich and B. D. Kilgore, PAGEOPH **143**, 283 (1994).
[15] P. Berthoud, T. Baumberger, C. G'Sell, and J. M. Hiver, Phys. Rev. B **59**, 14 313 (1999).
[16] C. Caroli and P. Nozieres, in *Physics of Sliding Friction*, edited by B. N. J. Persson and E. Tosatti (Kluwer, Dordrecht, 1996).
[17] G. Gudehus (private communication).